



Silver Nanoparticles Grown in Organic Solvent PGMEA by Pulsed Laser Ablation and Their Nonlinear Optical Properties

Hongfei Shi, Can Wang*, Yueliang Zhou, Kuijuan Jin*, and Guozhen Yang

*Beijing National Laboratory for Condensed Matter Physics, Institute of Physics,
Chinese Academy of Sciences, PO Box 603, Beijing 100190, P. R. China*

Well dispersed silver nanoparticles (AgNPs) with narrow size distribution have been grown in organic solvent propylene glycol monomethyl ether acetate (PGMEA) by pulsed laser ablation techniques. The presence of AgNPs in PGMEA solvent gives rise to an enhancement of the absorption and nonlinear optical properties due to the surface plasmon resonance induced by AgNPs. The shape and density of the AgNPs have been estimated by fitting the absorption spectra with a given model, and the results also show that an additional laser irradiation treatment can improve the monodispersity of the AgNPs and their nonlinear optical properties. The synthesis of AgNPs in PGMEA will facilitate adding AgNPs into organic functional materials especially for photoresist to modify their optical properties.

Keywords: Silver Nanoparticles (AgNPs), Propylene Glycol Methyl Ether Acetate, Laser Ablation, Nonlinear Optical Absorption.

1. INTRODUCTION

Silver nanoparticles (AgNPs) have wide range of applications in physics, chemistry and biology. For instance, AgNPs have been used in molecular ruler,¹ single molecular electronic devices,² bactericidal agent,³ lithography,⁴ and surface enhanced Raman spectroscopy (SERS).⁵ Traditional and commonly employed method to synthesis AgNPs is chemically reduction of Ag⁺. However, in this chemical method, additional surfactants are needed, and some hardly removable byproducts can be inevitably produced, which may affect the successive applications.⁶ Laser ablation of metals in liquids,⁷ as a method to prepare 'chemically clean' metal nanoparticles in liquids, has attracted many investigations. Mafune et al.⁸ have studied the structure and stability of AgNPs in aqueous solution containing sodium dodecyl sulfate (SDS). Amendola et al. have synthesized free gold⁹ and silver¹⁰ nanoparticles in various organic solvents including TMSO, THF, and CH₃CN. Other common organic solvents such as ethanol,¹¹ isopropanol,¹² and acetone¹³ have also been used for synthesizing metal nanoparticles.

Propylene Glycol Methyl Ether Acetate (PGMEA) as a good organic solvent is widely used in micro/nanofabrication as a photoresist thinner or general clean up solvent. Chemically clean metal nanoparticles fabricated in this polar solvent can be easily mixed into many organic materials including photoresists. By introducing metal nanoparticles, the optical properties of PGMEA solution or photoresist can be modified due to the surface plasmon resonances of the metal nanoparticles. The surface plasmon resonances are caused by the enhancement of the local electromagnetic field near the metal surface.¹⁴ The modified optical properties including the absorbance and nonlinear optical properties may be helpful to improve their functionality in the applications.

In this study, chemically clean AgNPs were synthesized directly in PGMEA solvent by laser ablation, and their optical properties were investigated. Ultraviolet-visible (UV-vis) absorption spectra and Transmission Electron Microscopy (TEM) images were employed to characterize the size distribution, aggregation and oxidation of the AgNPs. The spectra were fitted by the absorption theory to estimate the shape and concentration of the AgNPs in PGMEA. In addition, third order nonlinear optical susceptibility (χ^3) was investigated by using signal beam *z*-scan method.

*Authors to whom correspondence should be addressed.

2. EXPERIMENTAL DETAILS

Figure 1 illustrates the experiment configuration. Pulsed laser ablation was carried out with a Nd:YAG (Model: NL303G) Q-switch laser at 532 nm (duration: 8 ns, repetition rate: 10 Hz) focused by a 150 mm quartz lens on a silver plate immersed in PGMEA. Silver plate (99.9% pure) was washed with diluted HNO_3 and distilled water before being placed at the bottom of a 10 mm \times 10 mm fixed quartz cell containing 2 ml PGMEA. The light beam was adjusted to be perpendicular to the silver plate. After ablation, an unfocused laser beam was used to irradiate the colloid to investigate the irradiation effect on the nanoparticles.

Absorption spectra of the AgNP colloidal solutions were measured with a UV-vis spectrometer (SpectraPro-500i). To investigate the shape and size distribution of the AgNPs in detail, transmission electron micrographs of the AgNPs were obtained with a transmission electron microscope (JEOL JEM-2010). The samples for TEM study were prepared by casting a few drops of the colloid onto carbon-coated copper grids and then evaporating the solvent on a hot plate.

A typical single beam z -scan method¹⁵ was used to measure the real and imaginary parts of χ^3 . Laser beam from the Nd:YAG laser (repetition rate: 1 Hz) used in the ablation was attenuated, spatially filtered, and then focused with a 300 mm lens. Same quartz cell was used to carry the Ag colloids for the measurements. Before our measurements, a CS_2 sample was employed as a standard to calibrate the z -scan system.¹⁵ Moreover, no obvious nonlinear phenomenon of either the empty quartz cell or the pure PGMEA was observed at or even above the experimental laser intensity (approximately 10^7 W cm^{-2}).

3. RESULTS AND DISCUSSION

3.1. Absorption Spectra of Ablated AgNPs in PGMEA

Figure 2 shows absorption spectra of the AgNPs in PGMEA measured after different ablation times at 30 mW.

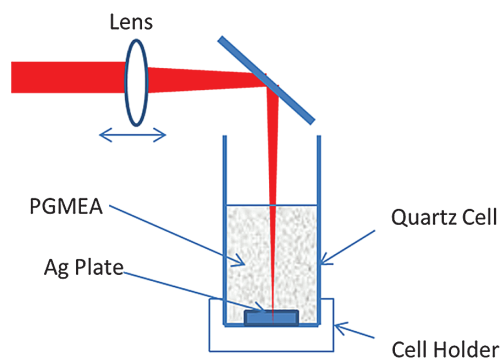


Fig. 1. Schematic diagram of the experimental apparatus.

The spectra of the AgNPs colloidal solutions have a characteristic peak around 400 nm which is caused by the surface plasmon resonance, and a tail of broad band toward UV region which is attributed to interband absorption. The surface plasmon peak of spherical AgNPs is sharp, but that of spheroid AgNPs is broadened, because of the simultaneous existence of longitude and transverse resonance mode. The peak position is correlated to particle size, shape, coating, and environment etc.¹⁴ Generally, the broad interband absorption around 250 nm is related to the concentration of AgNPs, so the intensity of this peak can be introduced to indicate the abundance of silver. Because of the large absorption of PGMEA below 260 nm, the absorbance at 260 nm rather than 250 nm was used to represent relative abundance.¹⁶ As ablation time increases, the relative abundance increases linearly as shown in Figure 2. Moreover, the peak also expands toward infrared region. This phenomenon can be explained by the existence of spheroids particles and particle aggregation.⁹ The efficiency of laser ablation is also affected by the power of the beam. It has been observed that the ablation using 150 mW for 5 min can obtain almost the same absorbance spectrum as using 30 mW for 35 min, so a 150 mW laser ablation for 10 min was chosen to ablate the AgNPs samples in this study.

3.2. Shape and Concentration of AgNPs in PGMEA

Extinction of small particles can be divided into absorption and scattering.¹⁷ For the AgNPs, in our consideration, the scattering can be neglected, so the extinction cross section is equal to the absorption cross section. Optical absorption spectra for silver spheres can be calculated using the Mie theory.¹⁸ The Mie theory solves the Maxwell equations in spherical coordinates under discontinuous boundary condition using multiples expansion of the electric and magnetic fields.¹⁸ For spherical particles much smaller than the electromagnetic wavelength, the dipolar approximation is valid and the cross section is in a simple analytic form. For

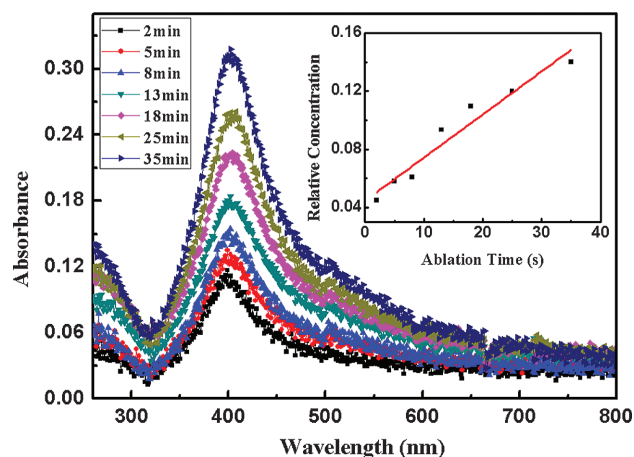


Fig. 2. Absorption spectra of the AgNPs colloids with different ablation time; Inset is the relative abundance's correlation between ablation time.

randomly oriented nonspherical particles, the cross section can be calculated using Gans model (or Mie-Gans theory), which is an extension of Mie model for spheroidal shapes under the dipolar approximation.

According to the Mie model, the extinction cross section of a spherical AgNP can be written as^{14,7}

$$\sigma_{\text{spherical}}(\omega) = 9 \frac{\omega}{c} \epsilon_m^{3/2} V \frac{\epsilon_2(\omega, R)}{[\epsilon_1(\omega, R) + 2\epsilon_m]^2 + \epsilon_2(\omega, R)^2} \quad (1)$$

Where $\epsilon_1(\omega, R)$ and $\epsilon_2(\omega, R)$ are the real and imaginary part of the dielectric constant of the particle respectively. ϵ_m is the dielectric constant of the medium. V is the volume of a single particle.

The aggregated AgNPs have a cigar-like shape, which can be modeled by prolate spheroids for first order approximation.⁹ For a prolate spheroid particle with three axis to be a, b , and c ($a > b = c$), according to the Gans model, the extinction cross section is^{9,14,17}

$$\begin{aligned} \sigma_{\text{spheroid}}(\omega) &= \frac{\omega}{3c} \epsilon^{3/2} V \\ &\times \sum_{j=a,b,c} \frac{\epsilon_2(\omega, R)/P_j^2}{[\epsilon_1(\omega, R) + ((1-P_j)/P_i)\epsilon_m]^2 + \epsilon_2(\omega, R)^2} \\ @ P_a &= \frac{1-e^2}{e^2} \left[\frac{1}{2e} \ln \left(\frac{1+e}{1-e} \right) - 1 \right] \end{aligned} \quad (2)$$

The distribution of aspect ratio a/b is assumed as Gaussian form:⁹

$$G(a/b) = \frac{1}{\sigma_G \sqrt{2\pi}} \exp \left[-\frac{(a/b-1)^2}{2\sigma_G^2} \right] \quad (3)$$

Where σ_G is the standard deviation of the aspect ratio a/b . It describes the degree of asymmetry between the two principle axes of spheroidal particles.

For a sample containing N AgNPs per volume, and with a thickness of L , the absorbance can be written as

$$A = \frac{NL((1-f)\sigma_{\text{spherical}} + f\sigma_{\text{spheroid}})}{\ln(10)} \quad (4)$$

Where f is the fraction of spheroids.

The contribution of spheroids can be described by two parameters:⁹ f , and σ_G . Along with another parameter of the mean radius R , which can be obtained from the TEM pictures (shown in Fig. 5), these three parameters are sufficient to describe absorption spectra. Detailed description of this model is presented in Ref. [9]. For the dielectric function of silver we use the published data in Ref. [19].

The diameter of the fresh AgNPs follows a lognormal distribution

$$f(x) = \frac{1}{x\sigma\sqrt{2\pi}} \exp \left(-\frac{(\ln(x/x_c))^2}{2\sigma^2} \right)$$

Where $x_c = 14.02$ nm and $\sigma = 0.611$ nm according to TEM picture in Figure 5(a). By fitting the absorption spectrum of the AgNPs colloid before irradiation in Figure 3 with the model mentioned above, we can get the best fitting at $f = 33.3\%$, $\sigma_G = 2.5$. This indicates that one third of the particles are spheroids with a large standard deviation of aspect ratio. By comparing the calculated spectrum to the measured, the concentration of the AgNPs in PGMEA is estimated to be around 5.2 $\mu\text{g/ml}$.

3.3. Irradiation Effect on AgNPs

An unfocused beam at 200 mW with the same parameters as the beam for the ablation was used to irradiate the colloid. As Figure 3 illustrates, after irradiation, the SP peak is enhanced, while the red end of the spectrum (475 nm–600 nm) is suppressed. Using the fitting method mentioned above, the best fitting of the spectrum after irradiation can be gotten at $f = 20.8\%$, $\sigma_G = 1.6$. The AgNPs got a lower fraction of spheroids and smaller standard deviation of aspect ratio. This is confirmed by the TEM pictures shown in Figure 5. Before irradiation, AgNPs are irregularly shaped and somewhat agglomerated together, but after irradiation AgNPs are more uniform and better separated. By analyzing the TEM images for hundreds of the AgNPs, the size distribution of the AgNPs is obtained as shown in Figure 6. Before irradiation, the size distribution follows the log-normal distribution in which smaller particles is the majority. But after irradiation, the size distribution follows the symmetrical Gaussian distribution, which means there is a size selection mechanism to diminish the number of small particles.

During irradiation, AgNPs would be vaporized and recrystallized.^{7,20} The spheroidal AgNPs could absorb more 532 nm laser energy than the spherical AgNPs, and

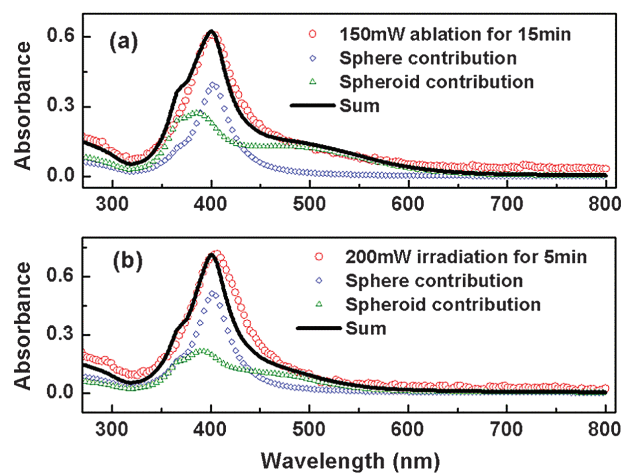


Fig. 3. Absorption spectra of the AgNPs colloids and their fitting curves before (a) and after (b) irradiation. Spherical and spheroid particles' contribution of each spectrum are also shown in the figure respectively.

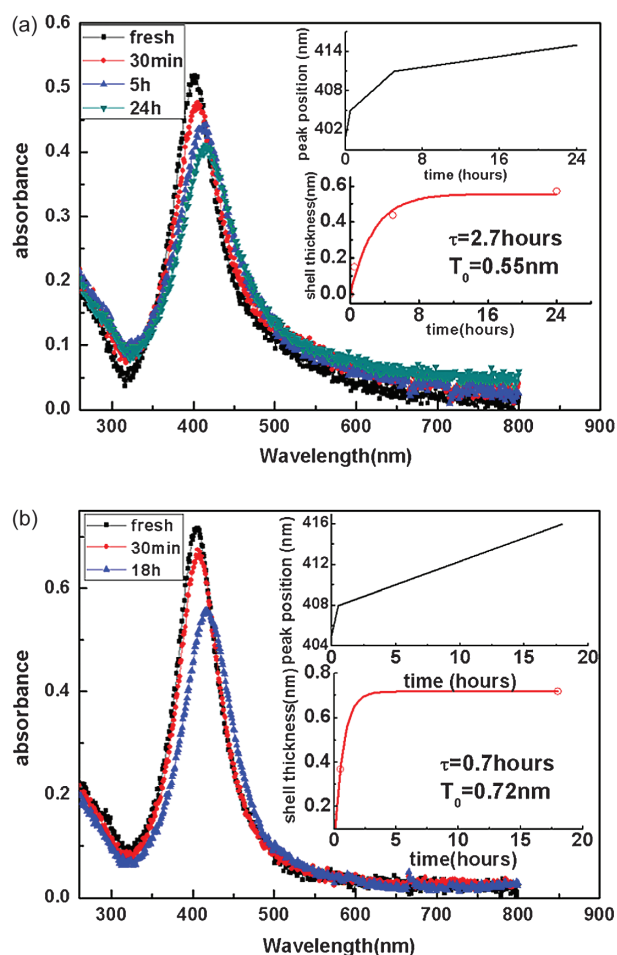


Fig. 4. Absorption spectra measured at different aging time for the AgNPs colloid before (a) and after irradiation (b). Insets show the variation of the peak position and shell thickness with aging time.

vaporize first to form more spherical shape because spherical particles are more stable. In conclusion, after irradiation, the spheroidal AgNPs can be changed to the spherical shape and this also induces the decrease in the absorbance at 532 nm.

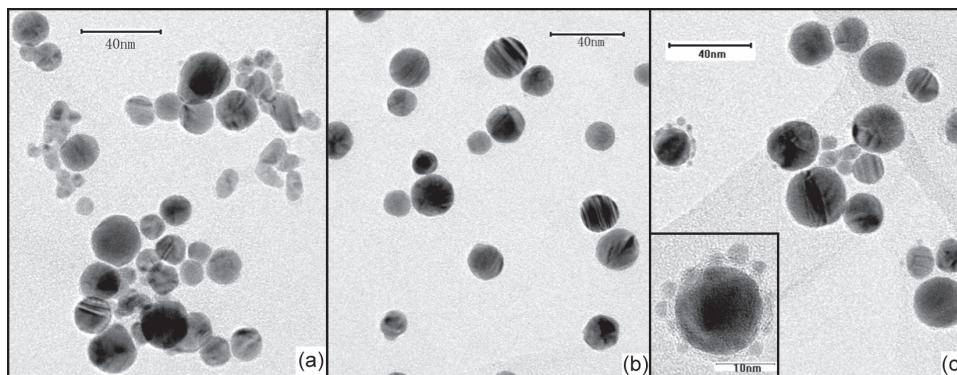


Fig. 5. TEM images for the AgNPs from the colloidal solutions: (a) before, (b) after irradiation, and (c) after aging for 4 days (Inset is a high resolution image showing the reaggregation).

3.4. Aging Effect of AgNPs

In general, AgNPs colloids should be used as early as possible after prepared, because aggregation or chemical reactions may happen in the colloidal solution with keeping time. So the aging effect of the AgNPs colloids has been investigated by absorption spectra and TEM observation. Figure 4 shows the absorption spectra measured at different aging time for the AgNPs colloids before and after irradiation. It can be observed that the SP peak decreases and shifts from 400 nm to 415 nm with aging time. The decrease of the SP peak can be attributed to the slight aggregation of the AgNPs after aging which is demonstrated by the TEM image shown in Figure 5(c). The red shift of the SP peak can be explained by introducing a shell layer of Ag₂O outside of the AgNPs.²¹ The insets of Figure 4 show the SP peak position and the calculated shell thickness with aging time.

Absorption cross sections of AgNPs with an Ag₂O coating can be calculated using the core-shell model.¹⁷ The extinction cross section is written as^{17,21}

$$\begin{aligned} \sigma \downarrow ([Ag] \downarrow 2O) &= 2\pi/\lambda 4\pi R \downarrow (\text{core} + \text{coating}) \uparrow 2 \\ &((\epsilon \downarrow ([Ag] \downarrow 2O) - \epsilon \downarrow m) \\ &(\epsilon \downarrow Ag + 2\epsilon \downarrow ([Ag] \downarrow 2O))) + \end{aligned} \quad (4)$$

Where $RT = R_{\text{coating}}/R_{\text{core+coating}}$ is the relative thickness of Ag₂O coating. For the dielectric constant of Ag₂O we use the published data in Ref. [22]. Using this model, the RT values for the sample at different aging times can be determined according to the position of the SP peak (Fig. 4).

As shown in Figure 4, thickness of Ag₂O shell T approaches a final thickness T_0 as time goes by. Thus, we set up a simple phenomenology model for the dynamic of oxidation:

$$\frac{dT}{dt} = (T_0 - T)/\tau \quad (5)$$

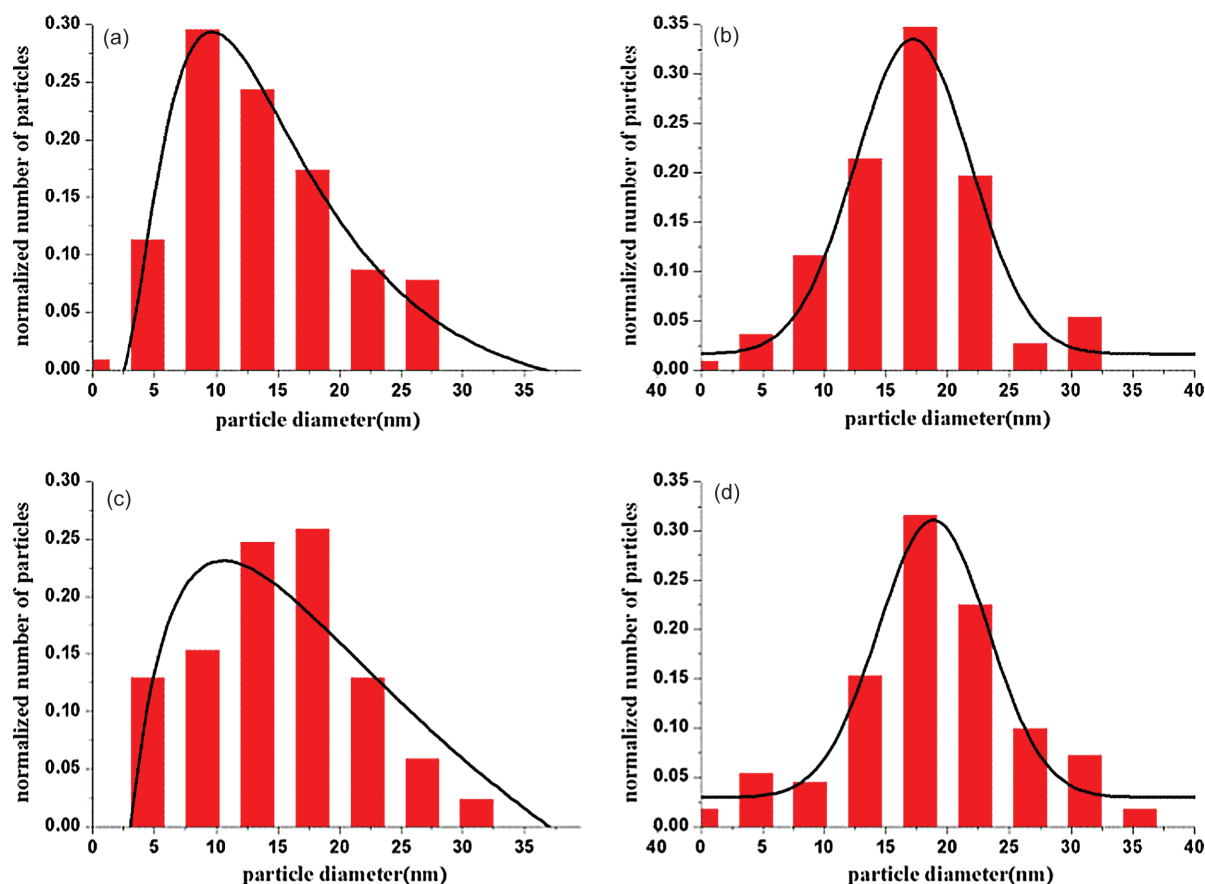


Fig. 6. The size distribution of the AgNPs from the colloids before and after irradiation without aging (a) and (b), and the colloids before and after irradiation with 4 hrs aging (c) and (d). (a) and (c) are fitted with log-normal curves and (b) and (d) are fitted with Gaussian curves.

And an empirical formula:

$$T = T_0 \left(1 - \exp\left(-\frac{t}{\tau}\right) \right) \quad (6)$$

T_0 reveals the final oxidation degree, while τ denotes the characteristic time of oxidation. Rendering data in Figure 4(b) to the formula above, we can get $T_0 = 0.55$ nm, $\tau = 2.7$ hr. for the sample before irradiation, and $RT_0 = 0.72$ nm, $\tau = 0.7$ hr. for the sample after irradiation. The final thickness of Ag_2O shell is slightly larger than the lattice constant of Ag_2O (0.47 nm). Therefore, nearly one unit cell layer of Ag_2O is formed with the characteristic oxidation time, and after that the thickness of the oxide layer keeps a constant T_0 . After irradiation, the final oxidation degree doesn't change significantly, but the characteristic time of oxidation is greatly shortened.

AgNPs as synthesized have no Ag_2O shell.²³ In 20 hours, both irradiated and none irradiated samples are oxidized significantly to form Ag_2O shells up to 0.7 nm. Therefore, to avoid the formation of the oxide layer, the AgNP colloids should be used as soon as possible after prepared.

3.5. Nonlinear Optical Absorption

Nonlinear optical susceptibilities of the AgNPs colloid were measured with z -scan method before and after the additional irradiation. Open aperture curves are represented in Figure 7, but closed aperture curves show no significant peak-valley feature. It means that the imaginary part of χ^3 dominates in the nonlinear optical properties of the colloid.¹⁵ Because no significant χ^3 is observed for the pure PGMEA, the nonlinear optical properties of the colloids should be induced by the AgNPs. Before irradiation, the value of $\text{Im}\chi^3$ for the AgNPs colloid is calculated to be 2.776×10^{-12} esu by fitting the open aperture curve using the thin sample model.^{15,24} The linear absorption coefficient α of the AgNPs colloid is 0.2524 cm^{-1} obtained from the UV-vis spectrum. A critical parameter that determines whether a nonlinear optical material can be used in applications is the figure of merit $FOM = |\chi^3|/\alpha$.²⁵ Ignoring the absorption of PGMEA at 532 nm, the FOM of the AgNPs colloid is about 1.1×10^{-11} esu cm. After an additional irradiation, the $\text{Im}\chi^3$, α , and FOM for the AgNPs colloid are determined to be 5.154×10^{-12} esu, 0.1257 cm^{-1} , and 4.1×10^{-11} esu cm, respectively. After the additional irradiation, $\text{Im}\chi^3$ is double increased and the FOM is four times of that before irradiation.

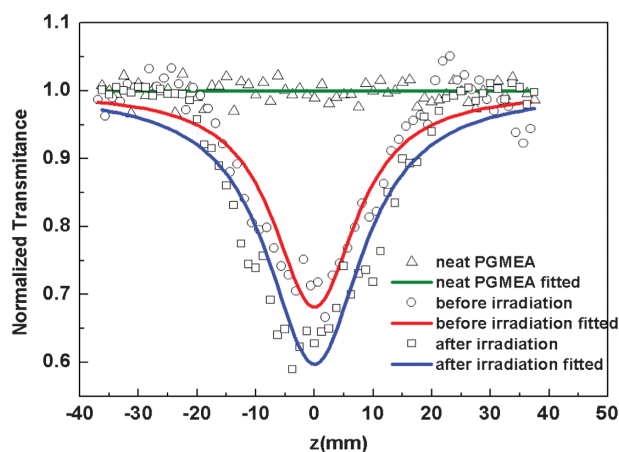


Fig. 7. Z-scan curves measured with open aperture for the pure PGMEA (open triangles), and the AgNPs colloids before (open circles) and after irradiation (open rectangle).

The amount of AgNPs would be maintained during irradiation, as there is no obvious change in the interband absorbance at 260 nm. But the size, shape, and the degree of aggregation of the AgNPs have been changed after irradiation, as shown in the TEM pictures in Figure 5. Therefore, the nonlinear optical properties of the AgNPs in PGMEA might be correlated to the morphology of the particles, and the monodisperse AgNPs would have better nonlinear optical properties. Shape dependence of nonlinear optical properties of gold nanoparticles have also been investigated by Dong et al.²⁶ Larger reverse saturation absorption (RSA) effect has been observed in icosahedron particles than cube and tetrahedron. It is obvious that icosahedron is more close to spherical and has a larger RSA effect. However, some reported works on the shape dependence of nonlinear optical absorption have also shown that the greater absorption cross section gives a larger RSA.²⁷

To explain this phenomenon, we have to investigate the effect on extinction spectrum of AgNPs caused by high energy laser. For the monodispersed AgNPs colloid, the SP peak has a narrow Lorenz line profile. But under high power laser, the peak shows redshift and broadening.²⁸ For spherical particles, SP peak is near 400 nm, and our operating wavelength is 532 nm, this lead to an increase of absorbance or RSA is expected which is consistent with our result. But, for spheroid particles, the longitude SP peak is near 500 nm,¹⁰ which has been confirmed by the absorption spectrum (Fig. 3). The red-shift of the longitude SP peak results in a decrease of absorption. This will raise a saturable absorption (SA) effect with a minus nonlinear absorption coefficient. Anyway, in this case, the contribution of spherical particles to nonlinear absorption coefficient is positive while spheroid particles negative. In our experiment, particles are more spherical after irradiation, then the contribution of RSA increases while

the contribution of SA is suppressed, thus the nonlinear absorption coefficient increases.

4. CONCLUSIONS

Chemically clean well-dispersed AgNPs were synthesized directly in organic solvent PGMEA by pulsed laser ablation. The shape and density of the AgNPs have been estimated by fitting the absorption spectra with a given model. The results show that the AgNPs in the solvent can modify the optical properties significantly by the surface plasmon resonance. An additional irradiation treatment can improve the monodispersity of AgNPs and reshape them to be more spherical, which gives rise to the increase of the RSA effect of AgNPs and the enhancement of the nonlinear optical properties subsequently. However, a single layer of Ag₂O coating outside of the Ag core could be formed within a few hours after synthesized, which may make against the use of AgNPs.

Acknowledgment: This work is supported by the National Key Basic Research Program of China under (Grant No. 2011CB301802) and the National Science Fund for Distinguished Young Scholars (Grant No. 10825418).

References and Notes

1. C. Sonnichsen, B. M. Reinhard, J. Liphardt, and A. P. Alivisatos, *Nat. Biotechnol.* 23, 741 (2005).
2. T. Dadosh, Y. Gordin, R. Krahn, I. Khivrich, D. Mahalu, V. Frydman, J. Sperling, A. Yacoby, and I. Bar-Joseph, *Nature* 436, 677 (2005).
3. S. K. Gogoi, P. Gopinath, A. Paul, A. Ramesh, S. S. Ghosh, and A. Chattopadhyay, *Langmuir* 22, 9322 (2006).
4. J. X. Huang, A. R. Tao, S. Connor, R. R. He, and P. D. Yang, *Nano Lett.* 6, 524 (2006).
5. L. L. Zhao, L. Jensen, and G. C. Schatz, *J. Am. Chem. Soc.* 128, 2911 (2006).
6. G. Schmid and B. Corain, *Eur. J. Inorg. Chem.* 3081 (2003).
7. G. W. Yang, *Prog. Mater. Sci.* 52, 648 (2007).
8. F. Mafune, J. Kohno, Y. Takeda, T. Kondow, and H. Sawabe, *J. Phys. Chem. B* 104, 9111 (2000).
9. V. Amendola, S. Polizzi, and M. Meneghetti, *J. Phys. Chem. B* 110, 7232 (2006).
10. V. Amendola, S. Polizzi, and M. Meneghetti, *Langmuir* 23, 6766 (2007).
11. G. Compagnini, A. A. Scalisi, and O. Puglisi, *Phys. Chem. Chem. Phys.* 4, 2787 (2002).
12. J.-S. Jeon and C.-S. Yeh, *J. Chin. Chem. Soc.* 45, 6 (1998).
13. M. Kawasaki and N. Nishimura, *Appl. Surf. Sci.* 253, 2208 (2006).
14. S. Link and M. A. El-Sayed, *J. Phys. Chem. B* 103, 8410 (1999).
15. M. Sheikbaha, A. A. Said, T. H. Wei, D. J. Hagan, and E. W. Vanstryland, *IEEE J. Quantum Electron.* 26, 760 (1990).
16. T. Tsuji, K. Iryo, Y. Nishimura, and M. Tsuji, *J. Photochem. Photobiol. A* 145, 201 (2001).
17. C. F. Bohren and D. R. Huffman, *Absorption and Scattering of Light by Small Particles*, Wiley, New York (1983).

18. G. Mie, *Annal. Physik* 25, 68 (1908).
19. P. B. Johnson and R. W. Christy, *Phys. Rev. B* 6, 4370 (1972).
20. J. Bosbach, D. Martin, F. Stietz, T. Wenzel, and F. Trager, *Appl. Phys. Lett.* 74, 2605 (1999).
21. J. M. J. Santillan, L. B. Scaffardi, and D. C. Schinca, *J. Phys. D Appl. Phys.* 44 (2011).
22. J. H. Qiu, P. Zhou, X. Y. Gao, J. N. Yu, S. Y. Wang, J. Li, Y. X. Zheng, Y. M. Yang, Q. H. Song, and L. Y. Chen, *J. Korean Phys. Soc.* 46, S269 (2005).
23. D. C. Schinca, L. B. Scaffardi, F. A. Videla, G. A. Torchia, P. Moreno, and L. Roso, *J. Phys. D Appl. Phys.* 42 (2009).
24. P. B. Chapple, J. Staromlynska, and R. G. McDuff, *J. Opt. Soc. Am. B-Opt. Phys.* 11, 975 (1994).
25. K. Uchida, S. Kaneko, S. Omi, C. Hata, H. Tanji, Y. Asahara, A. J. Ikushima, T. Tokizaki, and A. Nakamura, *J. Opt. Soc. Am. B-Opt. Phys.* 11, 1236 (1994).
26. J. Dong, X. Zhang, Y. Cao, W. Yang, and J. Tian, *Mater. Lett.* 65, 2665 (2011).
27. J. Z. Dong, X. L. Zhang, Y. A. Cao, W. S. Yang, and J. G. Tian, *Mater. Lett.* 65, 2665 (2011); C. Zheng, Y. H. Du, M. Feng, and H. B. Zhan, *Appl. Phys. Lett.* 93 (2008).
28. C. Voisin, N. Del Fatti, D. Christofilos, and F. Vallee, *J. Phys. Chem. B* 105, 2264 (2001).

Received: 24 February 2012. Revised/Accepted: 15 June 2012.